

## Magnetotransport through an antidot lattice in GaAs-Al<sub>x</sub>Ga<sub>1-x</sub>As heterostructures

K. Ensslin and P. M. Petroff

Materials Department, University of California, Santa Barbara, California 93106

(Received 12 February 1990)

Regular two-dimensional arrays of antidots with periodicities in the range of 200–500 nm are prepared in GaAs-Al<sub>x</sub>Ga<sub>1-x</sub>As heterostructures by means of Ga-focused ion-beam implantation. Transport measurements at low magnetic fields reveal a strong negative magnetoresistance originating from the localization of the electrons in the potential valleys between antidots. The low-temperature mobilities of the carriers deduced from the  $B=0$  resistance are in the range of 1000–30000 cm<sup>2</sup>/Vs. Under illumination mobility changes by more than a factor of 20 can be achieved. For high magnetic fields well-defined Shubnikov-de Haas oscillations and quantum Hall plateaus are observed. Close to  $B=0$  a very small structure in the magnetoresistance occurs reflecting the commensurability of the cyclotron diameter and the periodicity of the antidot array.

Low-dimensional quantum structures are of current interest in fundamental physics as well as in device engineering.<sup>1</sup> One-dimensional transport has been realized by various technologies<sup>2-4</sup> revealing intriguing results such as quantized conductance and ballistic transport through a narrow constriction. Zero-dimensional electronic behavior of quantum dots has been demonstrated by far-infrared spectroscopy,<sup>5</sup> resonant tunneling,<sup>6</sup> as well as capacitance techniques.<sup>7</sup> The transport through an array of quantum dots represents a difficult problem since the transport depends not only on the zero-dimensional (0D) subband structure itself but also very strongly on the thickness and the height of the barriers in between the quantum dots.

In this paper we use an antidot lattice,<sup>8</sup> where circularly damaged regions created by focused ion-beam implantation are surrounded by good-quality material of a molecular-beam-epitaxy (MBE) grown two-dimensional electron gas (2D EG). With decreasing periodicity of the antidots this allows us to study the transition from a 2D EG with a periodic array of scattering centers to an array of confined states, which arise from the overlap of the antidots. Using the persistent photoeffect, the carrier density  $N_s$  of the 2D EG and therefore the depletion length of the implanted antidots can be changed. This gives us the possibility to change the Drude mobility of the implanted material by more than a factor of 20. For low magnetic fields ( $B < 0.5$  T) we observe a pronounced negative magnetoresistance due to the localization of the carriers, leading to an estimate for the localization length as well as for the depletion length of the implanted regions. Furthermore, for  $N_s > 2 \times 10^{11}$  cm<sup>-2</sup> a small resistance oscillation arises from the commensurability of the cyclotron diameter  $2R_c$  and the periodicity  $p$  of the antidot lattice. For high magnetic fields, where  $2R_c \ll p$ , the transport is dominated by well-defined Shubnikov-de Haas (SdH) oscillations and broad quantum Hall plateaus.

The implanted GaAs-Al<sub>x</sub>Ga<sub>1-x</sub>As heterostructure is grown by molecular-beam epitaxy [growth sequence in Fig. 1(a)] and contains a 2D EG ( $N_s = 3 \times 10^{11}$  cm<sup>-2</sup>,  $\mu = 300000$  cm<sup>2</sup>/Vs at  $T = 4.2$  K) which is situated 300 nm below the surface of the sample to reduce the damage

created by the implanted ions. It has been shown in Ref. 9 that the ions channel up to 500 nm below the surface by conserving the beam diameter almost completely. Therefore the damaged area extends completely into the 2D EG, as indicated in Fig. 1(a). The mesa structure is a Hall geometry with four voltage probes on either side, as shown in Fig. 1(b). Only half the structure is implanted, allowing a direct comparison of the measurements on the implanted and nonimplanted regions. The implantation is carried out with single charged <sup>71</sup>Ga ions having an energy of 150 keV. The beam current is 4.2 pA, the typical

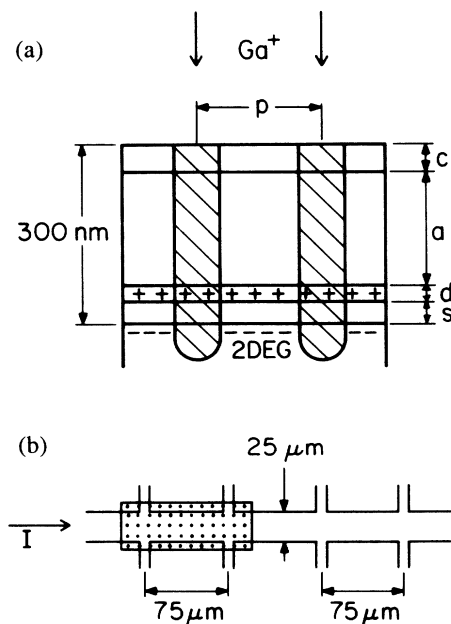


FIG. 1. (a) Schematic cross section of the as-grown sample. From the top: GaAs cap layer  $c = 8$  nm, Al<sub>x</sub>Ga<sub>1-x</sub>As ( $x = 0.3$ ) undoped layer  $a = 268$  nm, Al<sub>x</sub>Ga<sub>1-x</sub>As Si-doped ( $N_d = 10^{18}$  cm<sup>-3</sup>) layer  $d = 9$  nm, Al<sub>x</sub>Ga<sub>1-x</sub>As spacer layer  $s = 15$  nm. The shaded areas indicate the damage due to the Ga<sup>+</sup> implantation. (b) Schematic of the mesa-etched pattern. The dotted area indicates the implanted periodic antidot array.

spot size 80 nm, and the dwell time 800 ns. This leads to a dose of  $21 \text{ Ga}^+$  ions per antidot or an equivalent dose of  $3.3 \times 10^{11} \text{ cm}^{-2}$  in the region of the antidot for large values of  $p$ , where there is no overlap between the antidots. After implantation the samples are annealed at  $700^\circ\text{C}$  for 1 min in forming gas atmosphere.

The dc transport measurements are performed in a superconducting magnet (0–10 T) at liquid He temperatures  $T = 4.2 \text{ K}$ . The magnetic field  $B$  is oriented perpendicular to the plane of the 2D EG. Since the implanted regions of the samples are highly resistive (up to  $1 \text{ M}\Omega$  for low carrier densities, care is taken to avoid heating of the electrons by using very small currents, for some samples as low as 20 nA. The samples are cooled down in the dark. A red light-emitting diode (LED) is used to illuminate the samples and therefore change the carrier density  $N_s$  via the persistent photoconductivity effect. The time constants for the decay of the nonpersistent photo effect after switching off the LED are considerably longer (about a factor of 10) for the implanted material compared to the bare sample.

Figure 2 presents the results of the longitudinal magnetoresistance  $\rho_{xx}$  as a function of  $B$  for a sample implanted with an antidot array with periodicity  $p = 512 \text{ nm}$ . The uppermost curve is recorded without any illumination of the sample. For low magnetic fields,  $\rho_{xx}$  first drops, next passes a minimum at around  $B = 1 \text{ T}$ , and then increases continuously. This negative magnetoresistance arises

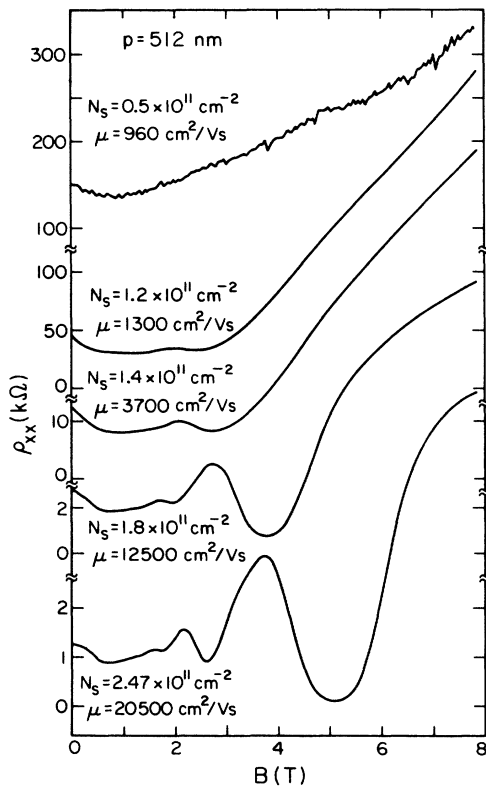


FIG. 2. Longitudinal magnetoresistance for a sample with  $p = 512 \text{ nm}$ . The traces from the top to the bottom of the figure are measured with increasing illumination. Note the big change in the scale of the ordinate for the different curves.

from the delocalization of the carriers as a function of  $B$ , as will be discussed later. The indicated carrier density of  $N_s = 0.5 \times 10^{11} \text{ cm}^{-2}$  is derived from the Hall resistance  $\rho_{xy}$ , which is a linear function of  $B$ . The Drude mobility  $\mu$  is obtained from  $\rho_{xx}(B=0)$ .

Illumination of the sample leads to an increase in  $N_s$ , as well as  $\mu$ . Furthermore, a series of minima in  $\rho_{xx}$  develops in addition to this first described minimum. An evaluation of the position of these minima as a function of  $1/B$  and a comparison with the carrier density  $N_s$  deduced from  $\rho_{xy}(B)$  clearly reveals that these oscillations are the SdH oscillations of the 2D EG. Within our measurement accuracy there is no detectable deviation from the  $1/B$  periodicity even for antidot arrays with  $p$  as low as  $p = 200 \text{ nm}$ . For the highest illumination state there is an additional structure in the drop of  $\rho_{xx}$  around  $B = 0.2 \text{ T}$ . The bump is related to the commensurability of the classical cyclotron diameter  $2R_c = 2(2pN_s)^{1/2} \hbar/eB$  and  $p$ . That effect has been discovered by Weiss *et al.*<sup>10</sup> and was explained by the formation of Landau bands<sup>11,12</sup> due to the superimposed lateral periodic potential. We like to point out the remarkable feature that the mobility  $\mu$  in the implanted region of the sample can be enhanced by more than a factor of 20 by simple illumination. At the same time the mobility in the bare nonimplanted sample only doubles from  $\mu = 300\,000 \text{ cm}^2/\text{Vs}$  to  $\mu = 600\,000 \text{ cm}^2/\text{Vs}$ .

Figure 3 shows  $\rho_{xx}$  together with  $\rho_{xy}$  for three samples with different periodicities  $p$ . The measured traces are chosen because the three samples have about the same carrier density  $(2.4\text{--}2.5) \times 10^{11} \text{ cm}^{-2}$ . However, the illumination time for the three samples differs significantly. The smaller  $p$ , the more photons are necessary to establish a given value of  $N_s$ . We conclude that the antidots not only act as scattering centers leading to a decrease from  $\mu = 300\,000 \text{ cm}^2/\text{Vs}$  (bare sample) to  $\mu = 1000 \text{ cm}^2/\text{Vs}$  (implanted sample,  $p = 512 \text{ nm}$ ) in the dark, but also trap a certain number of electrons, leading to a decrease in  $N_s$ . This also follows from the fact that for the nonilluminated sample with  $p = 512 \text{ nm}$  the carrier density in the bare sample is  $N_s = 3 \times 10^{11} \text{ cm}^{-2}$ , whereas the implanted sample has a much lower  $N_s = 0.5 \times 10^{11} \text{ cm}^{-2}$ . A simple calculation reveals that about 31 electrons are trapped per implanted  $\text{Ga}^+$  ion. The deduced values for  $\mu$  for the three curves in Fig. 2 differ greatly, whereas the quality of the SdH oscillations as well as of the Hall plateaus are comparable. Again additional shoulders on the low-field resistance are observed, shifting in agreement with the positions of the arrows being calculated by the condition  $2R_c = p$ , i.e.,  $B = 2(2pN_s)^{1/2} \hbar/ep$ .

In 1D wires negative magnetoresistance has been observed<sup>2,13,14</sup> and was successfully explained by the weak localization of the electrons.<sup>15,16</sup> In our case, due to the different dimensionality of our system, these theories are not valid. Neither is it possible to describe our results by the 2D localization theory,<sup>17</sup> which does not consider the periodicity and for small values of  $p$  also the additional confinement of the carriers. The question whether this negative magnetoresistance is due to weak localization effects or due to inhomogeneities induced by the implanted ions remains to be solved and will be clarified in future investigations. Hence we evaluated the localization be-

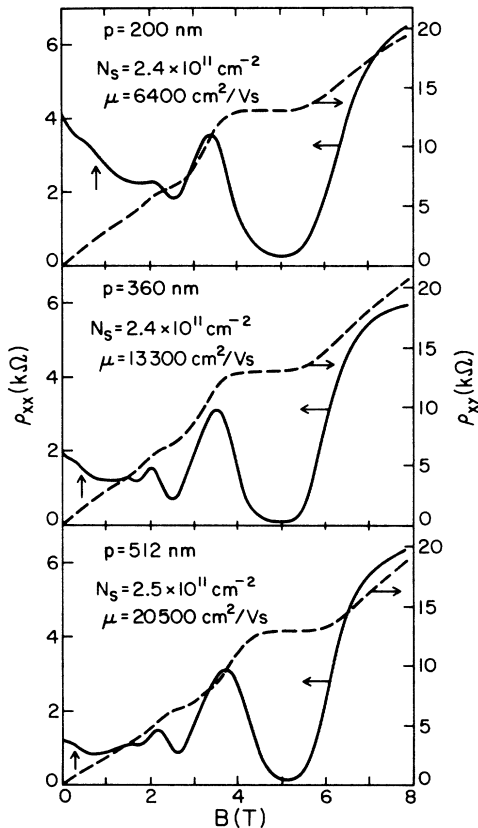


FIG. 3. Longitudinal (left-hand scale) and transverse (right-hand scale) magnetoresistance for three different periodicities of the antidot array. The curves are chosen, because they represent samples with different  $p$  values but comparable carrier densities.

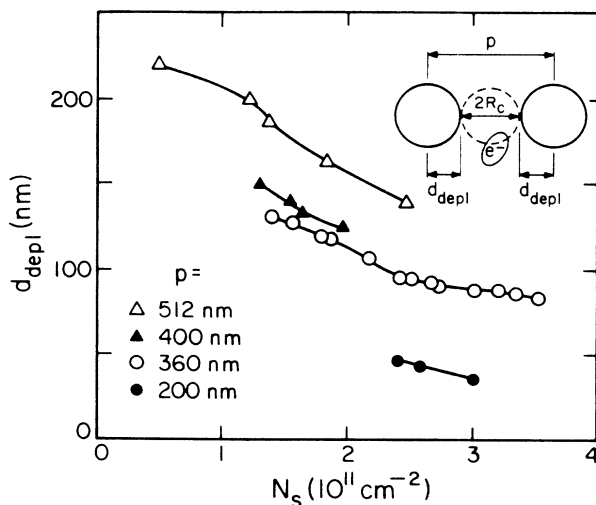


FIG. 4. Evaluated depletion length as a function of carrier density for samples with different periodicities of antidots. The smaller the  $p$ , the higher the density of trapping centers and thus the more photons that are necessary to achieve a certain value of  $N_s$ . The decrease of  $d_{\text{depl}}$  with decreasing  $p$  is therefore mainly due to the high-illumination powers for small values of  $p$ . The inset in the upper right-hand corner of the figure shows the concept of the geometrical consideration leading to an estimate for the depletion length.

havior in a more phenomenological way. We assume, that the minimum in  $\rho_{xx}$  in the low-field regime (SdH minima are not considered) is reached when the cyclotron diameter fits within the effective width between two antidots. This concept is sketched schematically in the inset of Fig. 4. We can thus give an upper limit for the depletion length  $d_{\text{depl}}$  of the carriers, following the relation  $(2d_{\text{depl}} + 2R_c) = p$ . Figure 4 summarizes the data obtained in this way for different values of  $p$ . As mentioned earlier the illumination dose to achieve a given value of  $N_s$  in the implanted material depends strongly on the number of trapping centers, i.e., the periodicity  $p$  of the antidots. Figure 4 clearly indicates that the depletion length  $d_{\text{depl}}$  decreases with increasing  $N_s$  for all values of  $p$ . With increasing  $N_s$  the screening behavior of the 2D EG is improved, and in addition more DX centers in the depletion region of the antidots are ionized, leading to an extension of the 2D EG in these regions, because the electrons are attracted by the newly created positive charges. These two effects qualitatively explain the decrease in  $d_{\text{depl}}$ . We conclude from Fig. 4 that we can realize antidots with  $d_{\text{depl}} < 50$  nm.

We use the usual expression for the depletion length<sup>18</sup>

$$d_{\text{depl}} = \left( \frac{2\epsilon_0\kappa\Delta E}{N_F e^2} \right)^{1/2},$$

where  $\Delta E$  is the value of the energy pinning ( $=E_g/2$  for free GaAs surfaces), and  $N_F$  the volume concentration of charges. For the observed value of  $d_{\text{depl}} = 50$  nm and an estimated  $N_F = 10^{16}$  cm<sup>-3</sup> we find for the energy pinning in our antidot system  $\Delta E = 19$  meV. Consequently, the potential in between the two well-separated antidots is given by two half parabolas connected by a straight line. As the periodicity  $p$  decreases, the length of the approximately straight line segment of the interantidot potential decreases. The interantidot potential becomes a complete parabola in the limit of this segment shrinking to zero. This kind of potential has been realized in so called 3D electron gases. It has been shown<sup>19</sup> that this parabolic potential is screened out by an increasing number of charges. In the present case the height of the potential  $\Delta E$  is comparable to the Fermi energy of the electrons. Thus the electrons can screen out part of the depletion length. For free GaAs surfaces the value of  $\Delta E$  is more than an order of magnitude larger, resulting in a value of  $d_{\text{depl}}$  almost independent of  $N_s$ . In the present case however, by extrapolating for a given value of  $N_s$  the  $d_{\text{depl}}$  vs  $p$  dependence we find a zero depletion width when the period  $p$  is about equal to the beam diameter. This tells us in agreement with the previous argument, that we can realize very small values of  $d_{\text{depl}}$ .

For high magnetic fields the value of  $N_s$  deduced from the periodicity of the SdH oscillations represents the carrier density between the antidots, in agreement with the low-field Hall effect (see Fig. 3). To check the nature of the scattering centers we extrapolate the low-field Hall effect and find that the Hall plateaus are slightly shifted to lower magnetic fields with respect to this extrapolated line. According to the experiments by Haug *et al.*,<sup>20</sup> this

indicates the presence of attractive scattering centers, in agreement with the observed trapping of carriers.

In conclusion, we present magnetotransport investigations on periodic arrays of antidots fabricated by Ga<sup>+</sup> focused ion-beam technology. At low magnetic fields a negative magnetoresistance is observed which enables us to deduce a depletion length smaller than 50 nm for an array with  $p=200$  nm. The  $B=0$  Drude mobility of the electrons can be changed by illumination by more than a fac-

tor of 20. At high magnetic fields well-defined SdH oscillations and quantum Hall plateaus are observed.

It is a pleasure to thank H. Kroemer, A. C. Gossard, A. Wixforth, F. Laruelle, G. Timp, D. Weiss, M. Miller, and J. H. English for valuable discussions and help in the experiments. We acknowledge financial support by the Air Force and "Quest," a National Science Foundation Science and Technology Center.

<sup>1</sup>For a recent review, see *Physics and Technology of Submicron Structures*, edited by H. Heinrich, G. Bauer, and F. Kuchar, Springer Series in Solid State Sciences Vol. 83 (Springer-Verlag, Berlin, 1988).

<sup>2</sup>T. J. Thornton, M. Pepper, H. Ahmed, D. Andrews, and G. J. Davies, *Phys. Rev. Lett.* **56**, 1198 (1986).

<sup>3</sup>B. J. van Wees, H. van Houten, C. W. J. Beenakker, J. G. Williamson, L. P. Kouwenhoven, D. van der Marel, and C. T. Foxon, *Phys. Rev. Lett.* **60**, 848 (1988).

<sup>4</sup>Y. Hirayama, T. Saku, and Y. Horikoshi, *Phys. Rev. B* **39**, 5535 (1989).

<sup>5</sup>Ch. Sikorski and U. Merkt, *Phys. Rev. Lett.* **62**, 2164 (1989).

<sup>6</sup>M. A. Reed, J. N. Randall, R. J. Aggarwal, R. J. Matyi, T. M. Moore, and A. E. Wetsel, *Phys. Rev.* **60**, 535 (1988).

<sup>7</sup>T. P. Smith III, K. Y. Lee, C. M. Knoedler, J. M. Hong, and D. P. Kern, *Phys. Rev. B* **38**, 2172 (1988).

<sup>8</sup>A similar structure was investigated by M. L. Roukes and A. Scherer, *Bull. Am. Phys. Soc.* **34**, 633 (1989).

<sup>9</sup>F. Laruelle, A. Bagchi, M. Tsuchiya, J. Merz, and P. M. Petroff, *Appl. Phys. Lett.* (to be published).

<sup>10</sup>D. Weiss, K. v. Klitzing, K. Ploog, and G. Weimann, *Euro-*

*phys. Lett.* **8**, 179 (1989).

<sup>11</sup>R. R. Gerhardts, D. Weiss, and K.v. Klitzing, *Phys. Rev. Lett.* **62**, 1177 (1989).

<sup>12</sup>R. W. Winkler, J. P. Kotthaus, and K. Ploog, *Phys. Rev. Lett.* **62**, 1177 (1989).

<sup>13</sup>T. Hiramoto, K. Hirakawa, Y. Iye, and T. Ikoma, *Appl. Phys. Lett.* **51**, 1620 (1987).

<sup>14</sup>T. Hiramoto, K. Hirakawa, Y. Iye, and T. Ikoma, *Appl. Phys. Lett.* **54**, 2103 (1989).

<sup>15</sup>B. L. Al'tschuler and A. G. Aronov, *Pis'ma Zh. Eksp. Teor. Fiz.* **33**, 515 (1981) [*JETP Lett.* **33**, 499 (1981)].

<sup>16</sup>C. W. Beenakker and H. van Houten, *Phys. Rev. B* **38**, 3232 (1988).

<sup>17</sup>S. Hikami, A. I. Larkin, and Y. Nagaoka, *Prog. Theor. Phys.* **63**, 707 (1980).

<sup>18</sup>T. Ando, A. B. Fowler, and F. Stern, *Rev. Mod. Phys.* **54**, 437 (1982).

<sup>19</sup>A. Wixforth, M. Sundaram, K. Ensslin, J. H. English, and A. C. Gossard, *Appl. Phys. Lett.* **56**, 456 (1990).

<sup>20</sup>R. J. Haug, R. R. Gerhardts, K.v. Klitzing, and K. Ploog, *Phys. Rev. Lett.* **59**, 1349 (1987).